Measurements

The number of progeny was highly variable between families and environments. Twenty-nine families consisting of 12 sires mated to 2 or 3 dams provided sufficient progeny (five male and five female) from all food treatments. Stored flies were sexed before measurement of eye-stalk length (median eye-stalk bristle to the centre of the head)[9] and wing length using a video camera mounted on a monocular microscope and the image analysis program NIH Image (Version 1.55). In addition thorax length was measured from the centre of the head to the lower edge of the thorax. All measurements were made 'blind' by a single person (T.B.). Two replicates of each measurement were taken on different days. Values were averaged over the left and right sides and the two replicates.

Statistical analysis

For each sex and each trait separately, a mixed-model ANOVA was evaluated with factors food quality (fixed), genotype (random; a genotype was defined as a full-sibling family) and the interaction[15]. As some families shared the same father, the analysis was repeated using hierarchical ANOVA with effects sire and dam-within-sire. Qualitatively similar relationships were found. The analysis was also carried out with pairs of environments to compute differences between environments, genetic correlation coefficients[15,16] and their standard errors[17]. Genetic correlation coefficients between environments are defined as the correlation between breeding values of the same genotype in two environments[16]. The equality of genetic variances between two environments was tested using Satterthwaite's method[15] based on the ratio $F = \frac{k_2 MS_{f,1} + k_1 MS_{e,2}}{k_1 MS_{f,2} + k_2 MS_{e,1}}$, where subscripts f and e refer to family and error mean squares, 1 and 2 to two environments, k_i to the number of replicates per family in environment i and MS to the mean squares. The approximate degrees of freedom for this F test are given in ref. 15. This ratio is constructed so that the denominator and the numerator have equal expectations when genetic variances are equal in both environments, even if error variance and sample sizes differ. For all traits and all environments, hierarchical ANOVAs with effects sire and dam-within-sire revealed no evidence of dominance or common environments as the dam component of variance was not significantly larger than the sire component[15,16]. So our estimates of r_a are not inflated by dominance or effects due to common environments. The analysis was repeated using relative trait values, with thorax length used as a general measure of body size. We used relative values rather than residuals. Analysis of residuals was more complex, as traits displayed changes in their allometric slopes and intercepts across environments. A full analysis using residuals reached the same conclusions (K.F. *et al.*, manuscript in preparation). Sample sizes were not the same for different traits because occasionally specimens exhibited damage to heads or wings. Given the number of tests performed, results with borderline significance ($0.01 < P < 0.05$) are treated with caution in our discussion.

Received 8 March; accepted 18 May 2000.

1. Andersson, M. Evolution of condition-dependent sex ornaments and mating preferences: sexual selection based on viability differences. *Evolution* **40,** 804–816 (1986).
2. Pomiankowski, A. Sexual selection: the handicap principle does work—sometimes. *Proc. R. Soc. Lond. B* **231,** 123–145 (1987).
3. Grafen, A. Biological signals as handicaps. *J. Theor. Biol.* **144,** 517–546 (1990).
4. Iwasa, Y. & Pomiankowski, A. The evolution of mate preferences for multiple handicaps. *Evolution* **48,** 853–867 (1994).
5. Rowe, L. & Houle, D. The lek paradox and the capture of genetic variance by condition dependent traits. *Proc. R. Soc. Lond. B* **263,** 1415–1421 (1996).
6. Hill, G. E. Proximate basis of variation in carotenoid pigmentation in male house finches. *Auk* **109,** 1–12 (1992).
7. Gustaffson, L., Qvarnström, A. & Sheldon, B. C. Trade-offs between life-history traits and a secondary sexual character in male collared flycatchers. *Nature* **375,** 311–313 (1995).
8. Hunt, J. & Simmons, L. W. Patterns of fluctuating asymmetry in beetles' horns: an experimental examination of the honest signalling hypothesis. *Behav. Ecol. Sociobiol.* **41,** 109–114 (1997).
9. David, P. *et al.* Male sexual ornament size but not asymmetry reflects condition in stalk-eyed flies. *Proc. R. Soc. Lond. B* **265,** 1–6 (1998).
10. Burkhardt, D. & de la Motte, I. Big 'antlers' are favoured: female choice in stalk-eyed flies (Diptera, Insecta), field collected harems and laboratory experiments. *J. Comp. Physiol. A* **162,** 649–652 (1988).
11. Wilkinson, G. S. & Reillo, P. R. Female choice response to artificial selection on an exaggerated male trait in a stalk-eyed fly. *Proc. R. Soc. Lond. B* **255,** 1–6 (1994).
12. Griffiths, S. C., Owens, I. P. F. & Burke, T. Environmental determination of a sexually selected trait. *Nature* **400,** 358–360 (1999).
13. Qvarnstrom, A. Genotype-by-environment interactions in the determination of the size of a secondary sexual character in the collared flycatcher (*Ficedula albicollis*). *Evolution* **53,** 1564–1572 (1999).
14. Wilkinson, G. S. & Taper, M. Evolution of genetic variation for condition-dependent traits in stalk-eyed flies. *Proc. R. Soc. Lond. B* **266,** 1685–1690 (1999).
15. Lynch, M. & Walsh, B. *Genetics and Analysis of Quantitative Traits* (Sinauer Associates, Sunderland, Massachussetts, 1998).
16. Roff, D. A. *Evolutionary Quantitative Genetics* (Chapman & Hall, London, 1997).
17. Falconer, D. S. & Mackay, T. F. C. *Introduction to Quantitative Genetics* 4th edn (Longman, Harlow, 1996).

Acknowledgements

We thank T. Chapman and G. Hurst for comments, and A. Hingle for help in rearing fly stocks. This work was supported by Royal Society university research fellowships (K.F. and A.P.) and the NERC.

Correspondence and requests for materials should be addressed to A.P. (e-mail: ucbhpom@ucl.ac.uk).

The segment polarity network is a robust developmental module

George von Dassow, Eli Meir, Edwin M. Munro & Garrett M. Odell

University of Washington, Department of Zoology, Box 351800, Seattle, Washington 98195-1800, USA

All insects possess homologous segments, but segment specification differs radically among insect orders. In *Drosophila*, maternal morphogens control the patterned activation of gap genes, which encode transcriptional regulators that shape the patterned expression of pair-rule genes. This patterning cascade takes place before cellularization. Pair-rule gene products subsequently 'imprint' segment polarity genes with reiterated patterns, thus defining the primordial segments. This mechanism must be greatly modified in insect groups in which many segments emerge only after cellularization[1]. In beetles and parasitic wasps, for instance, pair-rule homologues are expressed in patterns consistent with roles during segmentation, but these patterns emerge within cellular fields[2–4]. In contrast, although in locusts pair-rule homologues may not control segmentation[5,6], some segment polarity genes and their interactions are conserved[3,7–10]. Perhaps segmentation is modular, with each module autonomously expressing a characteristic intrinsic behaviour in response to transient stimuli. If so, evolution could rearrange inputs to modules without changing their intrinsic behaviours. Here we suggest, using computer simulations, that the *Drosophila* segment polarity genes constitute such a module, and that this module is resistant to variations in the kinetic constants that govern its behaviour.

Gap and pair-rule gene products are nuclear proteins that form short-range gradients in the *Drosophila* syncytial blastoderm, locally modulating each other's expression through direct transcriptional control. In contrast, segment polarity genes refine and maintain their expression state through a network of cross-regulatory interactions that require cell–cell communication[1–15]. Many segment polarity genes, unlike gap and pair-rule genes, remain active throughout development; the segment polarity network remembers the pattern imprinted upon it, then provides positional read-outs for subsequent developmental processes, including specification of neuroblasts, denticle patterns and appendage primordia. Thus, the intrinsic behaviour of the putative segment polarity module consists of stable, reiterated, asymmetric expression of its constituent genes, especially of the principal outputs *wingless* (*wg*), *hedgehog* (*hh*) and *engrailed* (*en*)[15]; in *Drosophila* the transient stimuli are pair-rule genes.

We used computer simulations to investigate whether the known interactions among segment polarity genes suffice to confer the properties expected of a developmental module. Given its probable conservation among diverse insects and perhaps beyond, we expected such a module to exhibit buffering against quantitative changes in gene function, and to be insensitive to the exact nature of input stimuli. We summarized (Box 1) the interactions among those segment polarity gene products that we reasoned might suffice to mimic the wild-type expression patterns of segment polarity genes (Fig. 1a). We abbreviated intermediate pathways and did not explicitly represent 'generic' components such as the transcriptional machinery. To formulate a dynamical model based on Box 1a required nearly 50 free parameters, including half-lives of messenger RNAs and proteins, binding rates, and cooperativity coefficients. The real values of these are unknown and the biologically realistic range for most parameters spans several orders of magnitude. Therefore we asked: is there any set of parameter values for

which the network model exhibits the desired behaviour, given realistic initial conditions?

Using only the solid lines in Box 1a we found no such parameter sets despite extensive efforts. Most randomly chosen parameter sets caused model components to oscillate strongly or caused some components to be expressed ubiquitously while others were repressed everywhere. Figure 1d shows the pattern most resembling the target, obtained for around 1 in 3,000 randomly chosen parameter sets from the initial pattern in Fig. 1b. No parameter sets produced stable asymmetric patterns. We realized that if Wg is the only input to *en* and Wg is secreted symmetrically from *wg*-expressing cells, expression of *en* must be activated in all neighbours. Similarly, as Hh signalling activates *wg* in neighbouring cells, *wg* must be expressed on either side of *en*-expressing cells. Thus, the solid connections in Box 1a cannot suffice to explain even the most basic behaviour of the segment polarity network. There must be both active repression of *en* in cells anterior to the *wg*-expressing stripe and something that spatially biases the response of *wg* to Hh. There is good evidence in *Drosophila* for *wg* autoactivation[16], and suggestive evidence that the Ci amino-terminal repressor fragment may inhibit *en*[17]. We incorporated these two possible remedies first (dashed lines, Box 1a). With these links installed there are many parameter sets that enable the model to reproduce the target behaviour, so many that they can be found easily by random sampling.

Each parameter set for which the model mimics Fig. 1a we call a 'solution' to the problem posed. Among 240,000 randomly-chosen parameter sets we found 1,192 solutions (~1 in 200). This is very frequent; as this search involved 48 parameters, on average a random choice of parameter value has roughly a 90% chance of being compatible with the desired behaviour (0.9^{48} is ~1/200). This holds even though most parameters range over several orders of magnitude. For comparison, if the model tolerated variation in the average parameter over 10% of its 100- or 1,000-fold range (a wildly optimistic expectation for a human-engineered electronic circuit), random search would find only one solution in 10^{48} samples. Figure 1e shows the stable pattern evolved for one such set of parameters from the pre-pattern in Fig. 1b. Clearly, under these conditions, the network model produces a pattern comparable to the target behaviour.

Figure 2a shows all 1,192 solutions found. Although some parameters cluster more tightly than others, none are confined to narrow sub-ranges. For each parameter, there is a solution for essentially any value. Thus, the network's ability to pass our test is intrinsic to its topology rather than to a specific quantitative tuning. There are so many diverse solutions that the notion of a globally optimal parameter set makes no biological sense. For instance, solutions for Wg diffusion rates (k_{MxferWG}, Fig. 2a) range over three orders of magnitude, from values allowing very little Wg traffic to values for which Wg diffuses rapidly across the segment.

To assess sensitivity to variation in individual parameters, we took parameter sets known to produce the desired behaviour and varied one parameter while holding all others fixed. In most cases, the model tolerates tenfold or more variation in the values of individual parameters (Fig. 3). In parameter space, abrupt transitions delineate zones within which the model behaves as desired from zones of qualitatively different behaviour. The canyons of working territory are sometimes narrow, but more often broad; the model often performs equivalently despite 100- or 1,000-fold variation in the value of some of the parameters. Thus, not only does the network topology embody many different solutions, but most solutions are highly robust to variation in individual parameter values.

Aside from patterns like Fig. 1e, the model has a complex repertoire, selected by initial conditions and parameter values. Many randomly sampled parameter sets lead to ubiquitous expression of some subset of model components and global repression of others. About 1 in 700 random sets evolves the degenerate pattern in Fig. 1d for the pre-pattern in Fig. 1b. Among the most common degenerate patterns are a one-cell-wide *wg* stripe overlayed by a three-cell-wide *en* strip, and a stripe of *en*-expressing cells surrounded by *wg*-expressing cells (~1 in 70 randomly chosen parameter sets each); the former pattern results for inadequate *en* repression and the latter from excessively avid *wg* autoactivation. Non-degenerate patterns include *en* and *wg* expressed in the same one-cell-wide stripe (~1 in

Box 1

A simple continuous dynamical model of the segment polarity gene network

a, Interactions among products of the five genes in our model: WG, wingless; EN, engrailed; HH, hedgehog; CID, cubitus interruptus (whole protein); CN, repressor fragment of cubitus interruptus; PTC, patched; PH, patched–hedgehog complex. Dashed lines were added according to the insufficiencies of the bold lines alone. Ellipses, mRNAs; rectangles, proteins; arrows, positive interactions; circles, negative interactions. ci is basally expressed (+ in rhombus). **b**, Examples of differential equations constituting our model. These simplified dimensional-form equations govern dynamics of hedgehog mRNA, protein and the Ptc-Hh complex; several terms (hh repression by CN, transport fluxes) have been left out for clarity. See Supplementary information for further details. **c**, Simple dose–response curve governing transcriptional activation (brackets in **b**), illustrating parameterization of the model. Transcription rate saturates because of inherent limits on how fast RNA polymerase can move ($T_{\max}$) multiplied by a gene-specific efficiency parameter (ρ_{hh}). for every monotonic regulator there is some concentration at which it has a half-maximal effect on its target (κ_{ENhh}). Each such interaction may exhibit non-linearity (ν_{ENhh}). In the case of cooperative binding, ν is equivalent to a Hill coefficient.

a

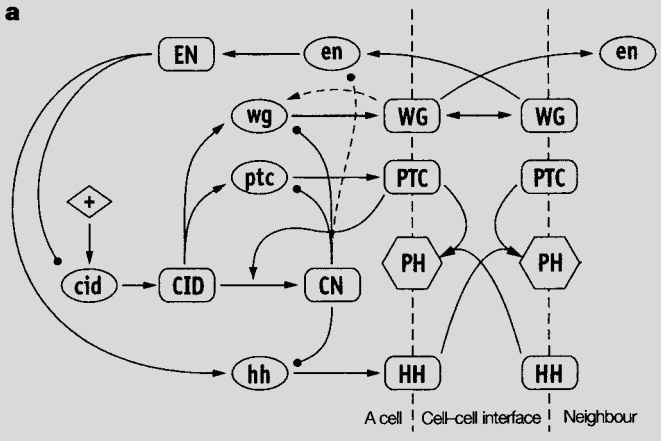

b

$$\frac{d[hh]_i}{dt} = T_{\max}\rho_{hh}\left[\frac{[EN]_i^{\nu_{ENhh}}}{K_{ENhh}^{\nu_{ENhh}} + [EN]_i^{\nu_{ENhh}}}\right] - \frac{[hh]_i}{H_{hh}}$$

$$\frac{d[HH]_{i,j}}{dt} = \frac{P_{\max}\sigma_{HH}[hh]_i}{6} - \frac{[HH]_{i,j}}{H_{HH}} - k_{PTCHH}[HH]_{i,j}[PTC]_{n,j+3}$$

$$\frac{d[PH]_{i,j}}{dt} = k_{PTCHH}[HH]_{n,j+3}[PTC]_{i,j} - \frac{[PH]_{i,j}}{H_{PH}}$$

c

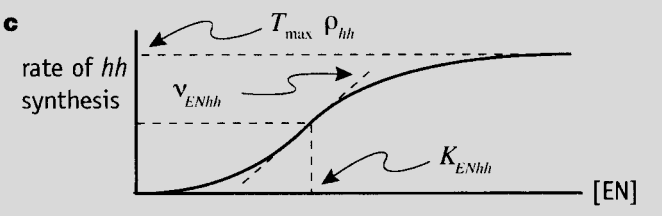

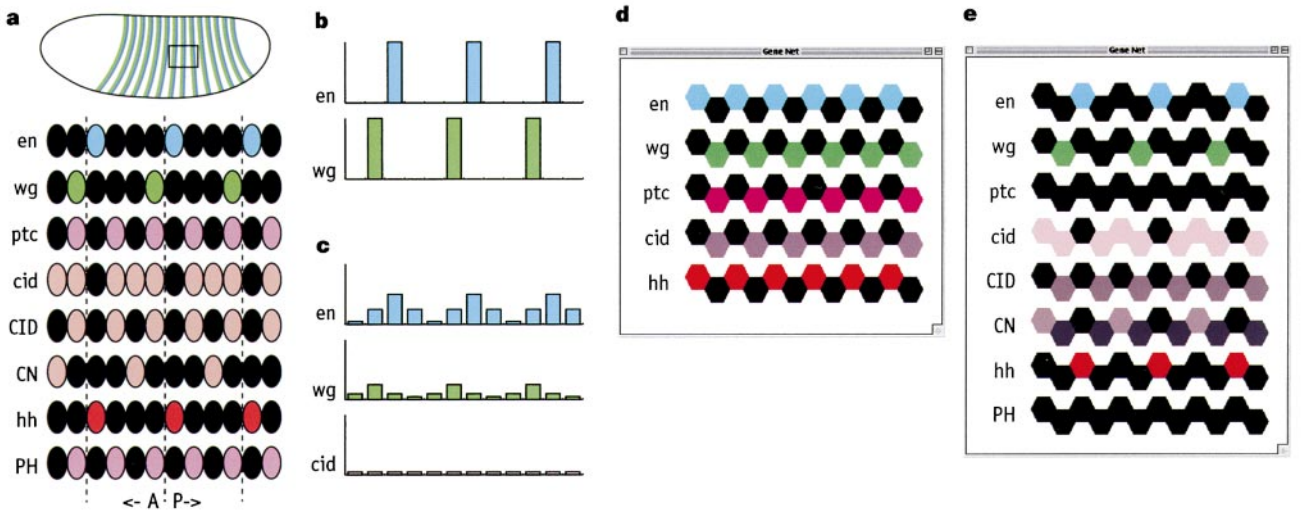

Figure 1 Segment polarity gene expression in *Drosophila*, pattern from wild type and several computer generated 'solutions'. **a**, Parasegmental boundaries divide columns of *wg*-expressing cells (green) from columns of *en*-expressing cells (blue). **b**, 'Crisp' initial conditions: *wg* activated in every fourth cell, *en* immediately posterior. Wg and En proteins are pulsed initially in the same pattern. **c**, 'Degraded' initial pattern. **d**, Best pattern achieved with solid lines in Box 1. **e**, Pattern achieved with dashed lines installed. For clarity we show a single strip of twelve cells; we impose repeating boundaries, so all cells have six neighbours no matter how many are in the field. Adding rows or columns has no effect.

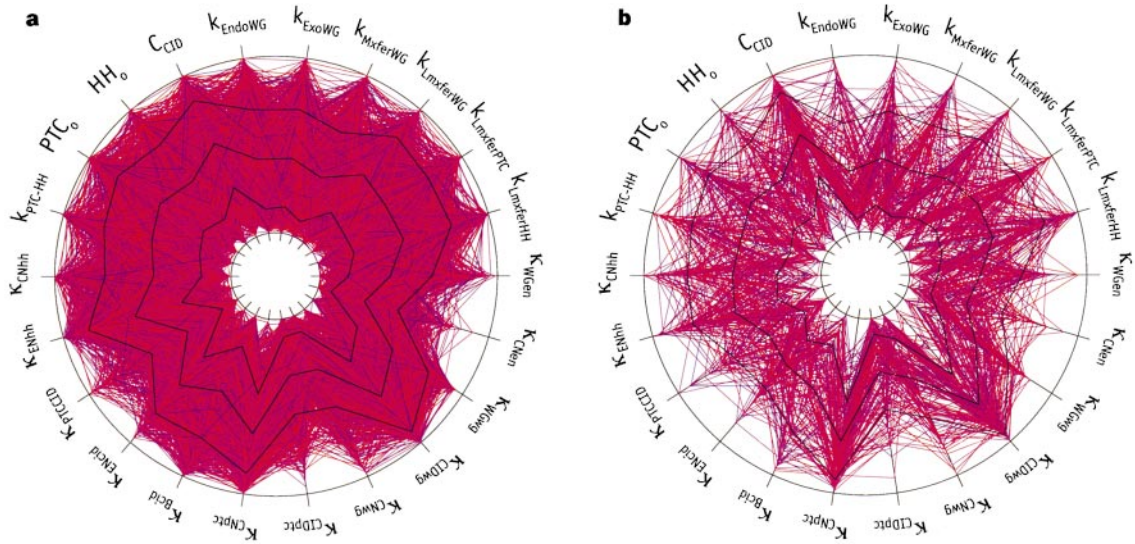

Figure 2 Graphic representation of 'solutions' obtained with crisp or degraded initial conditions. **a**, All 1,192 solutions found with crisp initial conditions. **b**, Solutions found with degraded initial conditions. Black lines plot mean and s.d. Each spoke represents the log-scale range of one parameter. Half-lives and cooperativity coefficients are omitted for clarity. Each polygon traces one parameter set as it intersects each spoke at the value of the indicated parameter. Polygons of extreme red intensity earned best scores; those of extreme blue intensity barely passed. For κ_{XXyy}, inner values represent potent regulation of *yy* by *XX*, outer values the opposite. For C_{CID} (cleavage of Ci), $k_{PTC\text{-}HH}$ (Ptc-Hh binding), $k_{MxferWG}$, $k_{LmxferWG}$ and similarly named (transfer processes), inner boundary means slow, outer means fast.

Table 1 Frequency of solutions as a function of initial conditions

Initial conditions	Minutes	Number of hits	Number of tries	Hit rate
Crisp: *wg*[2(h)]; Wg[2(h)]; *en*[3(h)]; En[3(h)]	200	1,192	240,000	1 in 201
Degraded: see Fig. 1c	600	149	750,000	1 in 5,000
Crisp, plus ubiquitous low-level *ci* and *ptc*: *ci*[1–4(l)]; *ptc*[1–4(l)]	200	110	41,258	1 in 375
Three-cell band of *ci*, stripe of *wg* on posterior margin: *wg*[2(h)]; *ci*[1(m),2(m),4(m)]	600	69	40,338	1 in 585
Three-cell band of *ptc*, stripe of *en* on anterior margin: *en*[3(h)]; *ptc*[1 m),3(m),4(m)]	600	127	36,196	1 in 285
Three-cell band of *ptc*, out-of-phase three-cell band of *ci*: *ci*[1(h),2(h),4(h)]; *ptc*-1(h),3(h),4(h)]	600	18	226,084	≥1 in 10^4
Close to target pattern: *wg*[2(h)]; Wg[2(h)]; *en*[3(h)]; En[3(h); *hh*[3(h)]; Hh[3(h)]; *ptc*[1(l),2(m)),4(m)]; Ptc[1(l)]; *ci*[1(m),2(m),4(m)]; Ci[1(l),2(m),4(m)], CiN75[1(m),2(l),4(l)]	200	464	21,526	1 in 46

Initial patterns coded relative to four-cell-wide segmental repeat, as in Fig. 1, with cells 1 and 2 anterior to and cells 3 and 4 posterior to the parasegmental boundary. Levels indicated as l, low (<20% of total possible); m, moderate (20–60% of total possible); h, high (60–100% of total possible). Thus, '*wg*[2(h)]' means a high level of wingless mRNA in cell 2. As indicated in the second column, all tests required acquisition of the target pattern within 200 min (for pre-patterns that contain both *wg* and *en* stripes) or 600 min plus stability over 1,000 min.

350) and *en* and *wg* expressed in overlapping three-cell-wide bands (~1 in 300). Although this is nowhere near a complete catalogue of the model's pattern-formation repertoire, these alternate regimes are among the 'near neighbours' of Fig. 1e in the sense that tuning parameters across the abrupt edges of canyons in Fig. 3 often yields these patterns.

We evaluated the model's sensitivity to initial conditions and discovered that the same stable pattern arises for a variety of input stimuli. The model has no 'wavelength'; that is, parameter values for which the model holds a four-cell-period repeat (Fig. 1e) enable it also to hold an equivalent three-, five- or arbitrary-period repeat pattern when triggered with a pre-pattern with corresponding spacing. We find that many solutions require only some initial bias towards expressing *wg* in one column, and *en* immediately posterior. Even for a very vaguely specified pre-pattern (Fig. 1c) we find solutions frequently (1 in 5,000)—still extremely high compared to the benchmark of 1 in 10^{48} cited above. Solutions for this case remain distributed throughout the parameter space (Fig. 2b). The model can achieve the target pattern with high frequency from initial conditions that do not include an initial pulse of *wg* or *en* (Table 1). Clearly, the model places few absolute demands on initial conditions, and it seems likely that the evolutionary process could replace inputs relatively easily.

With our model, we reconstituted *in silico* an aspect of biological behaviour from a subset of the known facts, much as a biochemist might reconstitute translation *in vitro*. Our reconstitution is far from complete. There are many additional segment polarity genes and many inputs to them. We simulated neither cell proliferation nor rearrangement, both of which affect the real network; additional components would help to integrate patterning with morphogenesis. Many segment polarity genes function as intermediate steps between components of our model or provide outputs to downstream targets. Despite its simplicity, our model illustrates a potentially valuable benefit of the general approach. Biologists' maps of gene networks are rapidly outgrowing our ability to comprehend genetic mechanisms using human intuition alone, as shown by our initial failure. Our results reveal holes in the current understanding of segmentation: what represses *en* anterior to the *wg*-expressing stripe, and what makes Hh signalling asymmetric? We incorporated the two simplest hypotheses here, but there are hints in the literature of other candidate mechanisms. In *Drosophila* the hole-filling utility of models is limited because developmental geneticists will probably fill in the holes fast enough without help from models. For other organisms (like humans) models may complement more limited experimental opportunities.

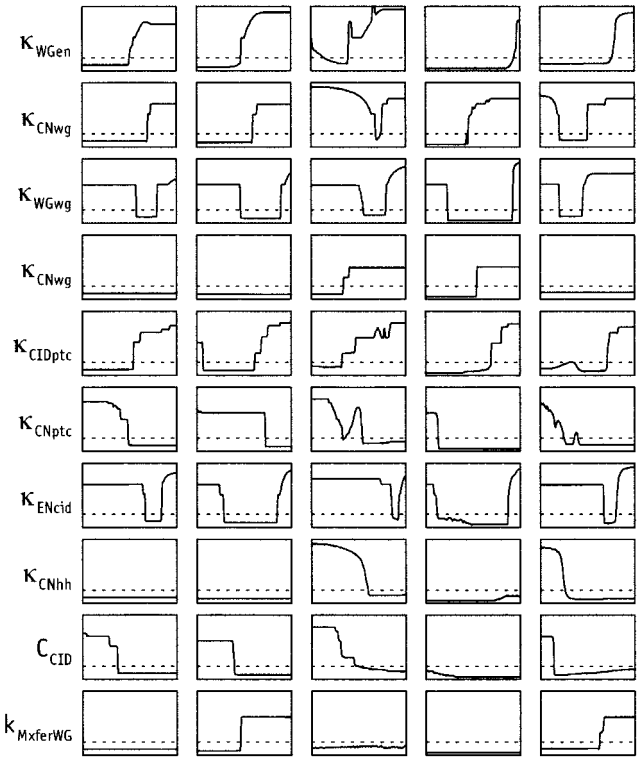

Figure 3 Sensitivity of individual solutions to varying individual parameters. Each column represents one solution, and rows are transects in which the named parameter varies while others are held fixed. The vertical axis is the goodness-of-fit score; lower scores are better matches. The dashed line indicates the boundary below which we accept the match. The horizontal axis is the parameter's log-scale range, three orders of magnitude for all. Columns one and two are typical. The third is an unusually brittle solution: κ_{CNen} and κ_{ENcid} can vary at most twofold. Column four shows the opposite extreme, and column five is a case with two working ranges for κ_{CIDptc} and κ_{CNptc}.

More importantly, computer simulations allow biologists to explore emergent systems-level properties of gene networks. Boolean networks and random directed graphs have been used to capture the 'statistical mechanics' of genetic systems[18]. Such idealizations allowed the exploration of enormously complex systems and the discovery of generic properties of ensembles of randomly wired networks. Many have used similar methods to capture specific biologically realistic behaviours, including developmental pattern formation in *Drosophila*[19]. Meanwhile, the use of continuous nonlinear dynamical systems has been advocated to express cell fate determination mechanisms and the maintenance of cell states[20]. Until recently this approach, which we take here, faced two obstacles: a paucity of facts about specific molecular mechanisms and limited computational power for solving nonlinear models. As these constraints evaporate, realistic dynamical models, based either on mass action or stochastic kinetics, will increase in usefulness. Slack foresaw that such tools would be most useful to the extent that complex genetic circuits decompose into quasi-autonomous subsystems, that is, modules[20]. Our work represents such a case. In another notable example, two models have been used to express the adaptive response of the bacterial chemotactic receptor, both concurring that the mechanism is highly robust[21,22].

The most striking systems-level property we report is the robustness to parameter variation. This is not an artefact of the wiring of our model. In work to be described elsewhere, we have analysed models that include additional links and components. Our conclusions hold for all biologically grounded variants as long as they retain the core topology shown in Box 1. Why should the segment polarity mechanism be so robust? Varying parameter values is proxy for mutations of small effect, and variation in initial conditions mimics one aspect of developmental 'noise'. We are exploring how much developmental noise embryos experience, which may explain why gene networks need buffering. Alternatively, in the evolution of segmentation there may have been pressure to neutralize mutations of small effect. We originally expected the core topology to be frail and easily perturbed, and expected to achieve robustness only by adding additional complexity; we expected the reconstitution approach to tell us which architectural features confer robustness. Confounding that expectation, the simplest model that works at all emerged complete with unexpected robustness to variation in parameters and initial conditions. □

Methods

Our model is a system of nonlinear ordinary differential equations, each characterizing the time-dependent change in concentration of one of the components of Box 1a in an indexed cell or cell face (see Supplementary Information for further details). All equations consist of either standard kinetic formulas or pseudo-steady-state approximations. Each generically includes three classes of additive term: a synthesis term, a first-order decay term, and zero or more terms representing transformation processes (heterodimerization or cleavage, for example) or flux between compartments (exocytosis or cell-to-cell traffic). We discretized diffusion according to cell faces: membrane-bound and extracellular molecules equilibrate at parameterized rates between adjacent faces of a cell, and

extracellular molecules equilibrate at parameterized rates between adjacent faces of a cell, and extracellular molecules also exchange from one cell's faces to the apposite faces of neighbouring cells.

We ran all simulations using a prototype (versions 0.62–0.66) of Ingeneue, a custom software package that we developed to construct and analyse models such as this. Ingeneue's core function is to parse a script describing a network like that in Box 1a, convert it internally into a system of differential equations, and then numerically solve the system while monitoring the time-dependent behaviour. For the network in Box 1a, each four-cell-wide by one-cell-high 'segment' repeat unit contributes 136 coupled equations that must be solved over a simulated time interval of hundreds to thousands of minutes. This calculation takes a few seconds on a desktop computer. We quantified the model's behaviour using a customized goodness-of-fit function that assigns a scalar score to each parameter set according to how well the model governed by that set matches the desired spatial pattern of gene expression within a set amount of time (typically 3 h) and holds it stably for a longer period (typically 15 h) (see Supplementary Information). Initial conditions, specified as starting concentrations, have no enforced persistence and are the only spatially heterogenous influence. Ingeneue searches parameter space, using either random sampling or nonlinear optimization algorithms, for sets of parameters that confer on the model the desired spatial pattern formation behaviour. Ingeneue is written in Java and runs on any computer platform for which a Java Virtual Machine v.1.1.7 or better is available. Software and model files are available from the authors at http://www.ingeneue.org

We composed Box 1a from the literature on segmentation in *Drosophila* as follows: Wg stimulates *en* transcription in neighbouring cells[23,24]; En promotes *hh* transcription[25] and represses *ci*[26]; Hh binds to and sequesters Ptc[27], decreasing the rate at which Ci is processed to form a repressor, CiN75[17], whereas CiN75 represses *wg* and *ptc*, full-length Ci activates these genes[17,28–30]; either Ci or CiN75 represses *hh*[29]; dashed lines indicate autoregulation of *wg* by an incompletely characterized pathway[16], and a suggested repressive effect of CiN75 on *en*. Also, *ci* is basally expressed. Not shown but included in the model are transcytosis and cell-to-cell diffusion of Wg; as Wg transfers from cell to cell, Wg produced in a particular cell can activate targets in that cell.

Received 14 October 1999; accepted 3 May 2000.

1. Patel, N. H. The evolution of arthropod segmentation: insights from comparisons of gene expression patterns. *Dev. Suppl.* 201–207 (1994).
2. Brown, S. J., Hilgenfeld, R. B. & Denell, R. E. The beetle *Tribolium castaneum* has a fushi tarazu homolog expressed in stripes during segmentation. *Proc. Natl Acad. Sci. USA* **91,** 12922–12926 (1994).
3. Grbic, M., Nagy, L. M., Carroll, S. B. & Strand, M. Polyembryonic development: insect pattern formation in a cellularized environment. *Development* **122,** 795–804 (1996).
4. Brown, S. J., Parrish, J. K., Beeman, R. W. & Denell, R. E. Molecular characterization and embryonic expression of the even-skipped ortholog of *Tribolium castaneum*. *Mech. Dev.* **61,** 165–173 (1997).
5. Patel, N. H., Ball, E. E. & Goodman, C. S. Changing role of even-skipped during the evolution of insect pattern formation. *Nature* **357,** 339–342 (1992).
6. Dawes, R., Dawson, I., Falciani, F., Tear, G. & Akam, M. Dax, a locust Hox gene related to fushi-tarazu but showing no pair-rule expression. *Development* **120,** 1561–1572 (1994).
7. Patel, N. H., Kornberg, T. B. & Goodman, C. S. Expression of engrailed during segmentation in grasshopper and crayfish. *Development* **107,** 201–212 (1989).
8. Brown, S. J., Patel, N. H. & Denell, R. E. Embryonic expression of the single *Tribolium* engrailed homolog. *Dev. Genet.* **15,** 7–18 (1994).
9. Nagy, L. M. & Carroll, S. Conservation of wingless patterning functions in the short-germ embryos of *Tribolium castaneum*. *Nature* **367,** 460–463 (1994).
10. Oppenheimer, D. I., MacNicol, A. M. & Patel, N. H. Functional conservation of the wingless-engrailed interaction as shown by a widely applicable baculovirus misexpression system. *Curr. Biol.* **9,** 1288–1296 (1999).
11. Akam, M. The molecular basis for metameric pattern in the *Drosophila* embryo. *Development* **101,** 1–22 (1987).
12. DiNardo, S., Sher, E., Heemskerk-Jongens, J., Kassis, J. A. & O'Farrell, P. H. Two-tiered regulation of spatially patterned engrailed gene expression during *Drosophila* embryogenesis. *Nature* **332,** 604–609 (1988).
13. Ingham, P. W., Baker, N. E. & Martinez-Arias, A. Regulation of segment polarity genes in the *Drosophila* blastoderm by fushi tarazu and even skipped. *Nature* **331,** 73–75 (1988).
14. Martinez Arias, A., Baker, N. E. & Ingham, P. W. Role of segment polarity genes in the definition and maintenance of cell states in the *Drosophila* embryo. *Development* **103,** 157–170 (1988).
15. DiNardo, S., Heemskerk, J., Dougan, S. & O'Farrell, P. H. The making of a maggot: patterning the *Drosophila* embryonic epidermis. *Curr. Opin. Genet. Dev.* **4,** 529–534 (1994).
16. Hooper, J. E. Distinct pathways for autocrine and paracrine Wingless signalling in *Drosophila* embryos. *Nature* **372,** 461–464 (1994).
17. Aza-Blanc, P., Ramirez-Weber, F. A., Laget, M. P., Schwartz, C. & Kornberg, T. B. Proteolysis that is inhibited by hedgehog targets Cubitus interruptus protein to the nucleus and converts it to a repressor. *Cell* **89,** 1043–1053 (1997).
18. Kauffman, S. A. *The Origins of Order: Self Organization and Selection in Evolution* (Oxford Univ. Press, New York, 1993).
19. Sanchez, L, van Helden, J. & Thieffry, D. Establishment of the dorso-ventral pattern during embryonic development of drosophila melanogaster: a logical analysis. *J. Theor. Biol.* **189,** 377–389 (1997).
20. Slack, J. M. W. *From Egg to Embryo: Determinative Events in Early Development* (Cambridge Univ. Press, New York, 1983).
21. Barkai, N. & Leibler, S. Robustness in simple biochemical networks. *Nature* **387,** 913–917 (1997).
22. Morton-Firth, C. J., Shimizu, T. S. & Bray, D. A free-energy-based stochastic simulation of the Tar receptor complex. *J. Mol. Biol.* **286,** 1059–1074 (1999).
23. Heemskerk, J., DiNardo, S., Kostriken, R. & O'Farrell, P. H. Multiple modes of engrailed regulation in the progression towards cell fate determination. *Nature* **352,** 404–410 (1991).
24. Vincent, J. P. & Lawrence, P. A. *Drosophila* wingless sustains engrailed expression only in adjoining cells: evidence from mosaic embryos. *Cell* **77,** 909–915 (1994).
25. Tabata, T., Eaton, S. & Kornberg, T. B. The *Drosophila* hedgehog gene is expressed specifically in posterior compartment cells and is a target of engrailed regulation. *Genes Dev.* **6,** 2635–2645 (1992).
26. Schwartz, C., Locke, J., Nishida, C. & Kornberg, T. B. Analysis of cubitus interruptus regulation in *Drosophila* embryos and imaginal disks. *Development* **121,** 1625–1635 (1995).
27. Chen, Y. & Struhl, G. Dual roles for patched in sequestering and transducing Hedgehog. *Cell* **87,** 553–563 (1996).
28. Alexandre, C., Jacinto, A. & Ingham, P. W. Transcriptional activation of hedgehog target genes in *Drosophila* is mediated directly by the cubitus interruptus protein, a member of the GLI family of zinc finger DNA-binding proteins. *Genes Dev.* **10,** 2003–2013 (1996).
29. Dominguez, M., Brunner, M., Hafen, E. & Basler, K. Sending and receiving the hedgehog signal: control by the *Drosophila* Gli protein Cubitus interruptus. *Science* **272,** 1621–1625 (1996).
30. Von Ohlen, T., Lessing, D., Nusse, R. & Hooper, J. E. Hedgehog signaling regulates transcription through cubitus interruptus, a sequence-specific DNA binding protein. *Proc. Natl Acad. Sci. USA* **94,** 2404–2409 (1997).

Supplementary Information is available on *Nature*'s World-Wide Web site (http://www.nature.com) or on http://www.ingeneue.org, or as paper copy from the London editorial office of *Nature*.

Acknowledgements

We acknowledge encouragement and support from D. Nasser and the NSF. E.M. was supported by a HHMI predoctoral fellowship.

Correspondence and requests for materials should be addressed to G.v.D. (e-mail: dassow@u.washington.edu).

A sphingosine-1-phosphate receptor regulates cell migration during vertebrate heart development

Erik Kupperman*, Songzhu An†, Nick Osborne*, Steven Waldron* & Didier Y. R. Stainier*

** Departments of Biochemistry and Biophysics and † Medicine, Programs in Developmental Biology, Genetics and Human Genetics, University of California San Francisco, San Francisco, California 94143-0448, USA*

Coordinated cell migration is essential in many fundamental biological processes including embryonic development, organogenesis, wound healing and the immune response. During organogenesis, groups of cells are directed to specific locations within the embryo. Here we show that the zebrafish *miles apart* (*mil*) mutation[1,2] specifically affects the migration of the heart precursors to the midline. We found that mutant cells transplanted into a wild-type embryo migrate normally and that wild-type cells in a mutant embryo fail to migrate, suggesting that *mil* may be involved in generating an environment permissive for migration. We isolated *mil* by positional cloning and show that it encodes a member of the lysosphingolipid G-protein-coupled receptor family. We also show that sphingosine-1-phosphate is a ligand for Mil, and that it activates several downstream signalling events that are not activated by the mutant alleles. These data reveal a new role for lysosphingolipids in regulating cell migration during vertebrate development and provide the first molecular clues into the fusion of the bilateral heart primordia during organogenesis of the heart.

We have taken a genetic approach to study organogenesis in vertebrates, specifically examining the morphogenetic events leading to heart formation. In all vertebrates, the myocardial progenitors involute early during gastrulation and come to occupy bilateral positions in the anterior lateral plate mesoderm (LPM). During somitogenesis, these cells undergo a second phase of migration toward the midline and fuse to form the definitive heart tube. Large-scale genetic screens in zebrafish have identified eight mutations